Journal of Computational and Applied Mathematics 294 (2016) 358–371

Contents lists available at ScienceDirect

Journal of Computational and Applied Mathematics

journal homepage: www.elsevier.com/locate/cam

Stability analysis of the marching-on-in-time boundary element method for electromagnetics

Elwin van 't Wout [a,b,*], Duncan R. van der Heul [b], Harmen van der Ven [a], Cornelis Vuik [b]

[a] National Aerospace Laboratory, Amsterdam, Netherlands

[b] Delft Institute of Applied Mathematics, Delft University of Technology, Delft, Netherlands

ARTICLE INFO

Article history:
Received 27 June 2014

Keywords:
Time-dependent boundary integral equations
Boundary element method
Variational formulation
Collocation
Stability

ABSTRACT

The Time Domain Integral Equation method for electromagnetics is an appealing computational method for many applications in industry. However, its applicability has long been suffering from instabilities. A rigorous analysis of the variational formulation is imperative to the successful design of stable and robust numerical schemes. In this paper, an established functional framework and stability theorem will be extended to the differentiated version of the electric field integral equations, which can be discretized more efficient and is more often used in engineering literature. The extended stability theorem, combined with efficiency requirements, will give guidelines on the choice of test and basis functions of the space–time Petrov–Galerkin scheme. A discrete equivalence with the collocation method results in the recommendation to choose the quadratic spline basis function in the standard Marching-on-in-Time scheme. Computational experiments confirm that the quadratic spline basis functions have superior stability characteristics compared to the conventional quadratic Lagrange basis functions in time.

1. Introduction

Computational methods for transient electromagnetic scattering phenomena have widespread applications in industry, for instance in the design of aircraft or microelectronic circuits. The use of a boundary integral equation method is an appealing choice, because the number of degrees of freedom scale quadratically with the electrical size of the object and no artificial boundary to truncate the computational domain is required. The formulation in time domain allows for efficient computations of wideband signals and the incorporation of nonlinear models for material characteristics. Nevertheless, the applicability of time-domain boundary integral equation (TDIE) methods to computational electromagnetics has been limited due to inefficiency and instability. With the development of computational accelerators based on plane-wave and fast Fourier transform techniques, large-scale structures have been simulated [1,2]. However, obtaining robust and stable simulations is still a major challenge.

Whereas the Galerkin discretization in space has been the *de facto* standard, no consensus has been reached yet on the numerical discretization in time. Collocation [1], space–time Galerkin [3] and convolution quadrature [4] are the most popular choices. In this paper, collocation, also called Marching-on-in-Time (MoT), will be used because of its efficiency and accuracy. However, this numerical scheme has a long history of instability and has defied many stabilization techniques.

* Correspondence to: Centre for Medical Image Computing, University College London, London, United Kingdom.
E-mail address: e.wout@ucl.ac.uk (E. van 't Wout).

http://dx.doi.org/10.1016/j.cam.2015.09.002
0377-0427/

Hence, stability of MoT schemes is an active topic of research [5–7] and this paper aims to provide a rigorous analysis of the stability of TDIE methods.

The instabilities encountered in TDIE methods can be subdivided into spectral and numerical instabilities. The spectral instabilities originate from the nontrivial null space of the continuous model equations, which consists of direct currents and resonances. These instabilities have successfully been eliminated with several techniques, for example Calderón preconditioning [8]. On the other hand, the numerical instabilities originate from the numerical discretization of the model equations and have been more persistent. These instabilities are typically noticed in simulations as exponentially increasing solutions that alternate on discrete time levels. Because the instability often plagues the solution only when the simulation time is long compared to the time scale of the excitation, it is also called late-time instability.

The model equations are given by retarded potential boundary integral equations and have a strong coupling of space and time. This prevents a straightforward use of classical stabilization techniques for ordinary and delayed differential equations. Remedies for numerical instability have to be specifically designed for TDIE methods. The most successful strategies are the following:

1. Suppression of high-frequency content: because the numerical instability is usually visible as a solution that alternates on discrete time levels, suppression of high-frequent content can alleviate the instability. This is the basis of filtering and averaging techniques [9], the use of large time step sizes [10] and the use of bandlimited temporal basis functions [11]. However, these techniques do not eliminate the instability entirely and impinge on efficiency and accuracy.
2. Improvement of numerical accuracy: as a boundary element method, the expressions of the elements of the discretization matrix contain surface integrals. Due to discontinuities in the integrand, standard quadrature techniques are inaccurate. The use of large CFL numbers [10], smooth temporal basis functions [12] and a separable approximation of convolutions [6] can improve the accuracy of evaluating the surface integrals. Furthermore, the use of quasi-exact integration techniques allows for very accurate evaluation of the elements of the discretization matrix and computational experiences confirm that this is necessary to obtain stability for MoT schemes [13,5,7].
3. Design of a functional framework: to obtain a stable numerical scheme, the solution of the variational formulation has to be bounded, which should be proven within a specific functional framework [14,15]. This is the most rigorous approach to eliminate numerical instability and will be adopted in this paper.

A thorough mathematical foundation for TDIE methods using space–time Galerkin discretization schemes has been given by Terrasse [16]. There, a functional framework for the time-domain Electric Field Integral Equation (EFIE) has been designed, based on the earlier work of Bamberger and Ha-Duong on scalar TDIE methods for acoustics [17]. The properties of the time-domain EFIE have been proven with a passage via the Laplace domain. This is also the approach commonly used in further research, see e.g. [18] for an overview. In this paper, the analysis of the TDIE method will be performed entirely in time-domain in order to stay close to the time-domain variational formulation that will be used to discretize the model equations. This makes the implications of the type of model equation on the choice of numerical scheme immediately visible.

In Terrasse [16], specific Sobolev spaces are designed such that uniqueness and boundedness of the solution of the variational formulation can be proven. This has been performed for the Electric Field Integral Equation (EFIE). The aim of this paper is to extend the stability theorem to the differentiated version of the EFIE. This version is broadly used in engineering literature and allows for more efficient discretization schemes [11,8,6]. However, the extended stability theorem cannot be applied directly to the efficient collocation scheme. This will be remedied by considering Petrov–Galerkin schemes that fit within the functional framework. These schemes will be shown to be discretely equivalent with collocation schemes with specific temporal basis functions. Since stability carries over to discretely equivalent schemes, an MoT scheme with quadratic spline basis functions that fits within the functional framework of the stability theorem will be used [19]. Computational experiments will confirm the stability.

2. Methodology

This paper focuses on the TDIE method, which is a boundary integral equation method in time domain for electromagnetic scattering analysis. The model equations, variational formulation, and the numerical discretization will be explained in Sections 2.1–2.3, respectively.

2.1. Model equations

Let us consider a bounded domain $\Omega^i \subset \mathbb{R}^3$ that represents the scatterer and $\overline{\Omega^i}$ its closure. The exterior domain $\Omega^e = \mathbb{R}^3 \setminus \overline{\Omega^i}$ represents free space. The unit outward normal vector $\hat{\mathbf{n}}$ on the interface $\Gamma = \partial\Omega^i = \partial\Omega^e$ points from Ω^i towards Ω^e. The scatterer is assumed to be a perfect electric conductor (PEC), for which the jump condition states that the tangential component of the electric field vanishes on the interface with free space. As initial condition, the incident wave field has not yet induced a current distribution on the scatterer at zero time. Then, the exterior scattering problem can be formulated as a boundary integral equation with the Stratton–Chu representation formula of Maxwell's equations, that is,

$$-\hat{\mathbf{n}} \times \hat{\mathbf{n}} \times \iint_\Gamma \left(\mu \frac{\dot{\mathbf{j}}(\mathbf{r}', \tau)}{4\pi R} - \frac{1}{\epsilon} \nabla \frac{\int_{-\infty}^{\tau} \nabla' \cdot \mathbf{J}(\mathbf{r}', \bar{t}) \mathrm{d}\bar{t}}{4\pi R} \right) \mathrm{d}\mathbf{r}' = -\hat{\mathbf{n}} \times \hat{\mathbf{n}} \times \mathbf{E}^i(\mathbf{r}, t) \tag{1}$$

for $(\mathbf{r}, t) \in \Gamma \times \mathbb{R}_+$. This is the Electric Field Integral Equation (EFIE) for a PEC object embedded in free space [1]. The distance between the observer and source location $\mathbf{r}$ and $\mathbf{r}'$ is denoted by $R = |\mathbf{r} - \mathbf{r}'|$. The dot notation $\dot{\mathbf{J}} = \frac{\partial}{\partial t}\mathbf{J}$ has been used to denote differentiation in time and ∇ and ∇' denote the surface nabla operator with respect to $\mathbf{r}$ and $\mathbf{r}'$, respectively. The EFIE has to be solved for the electric surface current density $\mathbf{J}(\mathbf{r}, t)$ for given incident electric field $\mathbf{E}^i(\mathbf{r}, t)$ and makes use of evaluation of the solution at the *retarded time level*

$$\tau = t - \frac{|\mathbf{r} - \mathbf{r}'|}{c}. \tag{2}$$

The speed of light is given by $c = (\epsilon\mu)^{-\frac{1}{2}}$ with ϵ and μ the permittivity and permeability of free space, respectively.

The EFIE contains an integral in time, which results in a dependency of the electric surface current at the present time level on its full time history. Computation and storage of the full time history is expensive. This can be alleviated by considering the time derivative of the EFIE, that is,

$$-\hat{\mathbf{n}} \times \hat{\mathbf{n}} \times \iint_\Gamma \left(\mu \frac{\ddot{\mathbf{J}}(\mathbf{r}', \tau)}{4\pi R} - \frac{1}{\epsilon} \nabla \frac{\nabla' \cdot \mathbf{J}(\mathbf{r}', \tau)}{4\pi R} \right) \mathrm{d}\mathbf{r}' = -\hat{\mathbf{n}} \times \hat{\mathbf{n}} \times \dot{\mathbf{E}}^i(\mathbf{r}, t). \tag{3}$$

Both model equations (1) and (3) are called EFIE in literature. To distinguish the two equations, they will be called the *original EFIE* and *differentiated EFIE*, respectively. Computational methods based on the differentiated EFIE are more efficient because the solution does not depend on the full time history but only a limited time history. On the other hand, the incident wave field has to be continuously differentiable for the differentiated EFIE, instead of continuity only for the original EFIE. Here, preference is given to efficiency with the use of the differentiated EFIE, as is done in most publications on TDIE methods.

2.2. Variational formulation

The variational formulation of the original EFIE considers the function space $\mathcal{H}^s$ that has been designed in [16]. Here, its definition and several important properties for the stability theorem will be summarized. Remember that the function space consists of space–time dependent, real-valued vector functions and that all definitions and properties in this section have been introduced in [16].

Definition 1. For E a Hilbert space, $\mathcal{D}'_+(E)$ denotes the space of distributions in $\mathbb{R}$ with values in E and zero for all $t < 0$, and $\mathcal{S}'_+(E)$ denotes the space of tempered distributions in $\mathcal{D}'_+(E)$. The space of Laplace transformable functions $LT(\sigma, E)$ is defined for $\sigma \in \mathbb{R}$ with $\sigma > 0$ as

$$LT(\sigma, E) = \left\{ f \in \mathcal{D}'_+(E),\ e^{-\sigma t} f \in \mathcal{S}'_+(E) \right\} \tag{4}$$

where $f = \mathbf{f}(\mathbf{r}, t)$ is a vector function depending on space and time.

The spatial component of the function space $\mathcal{H}^s$ will make use of divergence conforming surface functions. Specifically, the space $H^{-\frac{1}{2}}(\mathrm{div}, \Gamma)$ of boundary values of electromagnetic fields with finite energy is used [20]. The temporal properties of the function space $\mathcal{H}^s$ are most conveniently defined with a Fourier–Laplace transform.

Definition 2. For $\mathbf{f} \in LT(\sigma, E)$, the Fourier–Laplace transform is defined as

$$\widehat{\mathbf{f}}(\mathbf{r}, \omega) = \int_{-\infty}^{\infty} e^{i\omega t} \mathbf{f}(\mathbf{r}, t) \mathrm{d}t \tag{5}$$

for $\omega = \eta + i\sigma$, where i denotes the imaginary unit: $i^2 = -1$.

Definition 3. The function space $\mathcal{H}^s$ for $s \in \mathbb{R}$ is defined as

$$\begin{aligned} \mathcal{H}^s &= H^s_\sigma \left(\mathbb{R}_+, H^{-\frac{1}{2}}(\mathrm{div}, \Gamma) \right) \\ &= \left\{ \mathbf{f} \in LT\left(\sigma, H^{-\frac{1}{2}}(\mathrm{div}, \Gamma) \right),\ \ \|\mathbf{f}\|^2_{\sigma, s, -\frac{1}{2}\mathrm{div}} < \infty \right\} \end{aligned} \tag{6}$$

where

$$\|\mathbf{f}\|^2_{\sigma, s, -\frac{1}{2}\mathrm{div}} = \frac{1}{2\pi} \int_{-\infty+i\sigma}^{+\infty+i\sigma} |\omega|^{2s} \left\| \widehat{\mathbf{f}}(\cdot, \omega) \right\|^2_{H^{-\frac{1}{2}}(\mathrm{div}, \Gamma)} \mathrm{d}\omega \tag{7}$$

for $\sigma \in \mathbb{R}$ positive: $\sigma > 0$.

The function space $\mathcal{H}^s$ is a Hilbert space and a special case of a Sobolev space. Furthermore, the norm can be related to the energy of an electromagnetic field and corresponds to an inner product that is weighted in time.

Definition 4. For $(\mathbf{f}\times\hat{\mathbf{n}})\in\mathcal{H}^s$ and $\mathbf{g}\in\mathcal{H}^{-s}$, the inner product is defined as

$$\langle\mathbf{f},\mathbf{g}\rangle_\sigma=\int_{\mathbb{R}}e^{-2\sigma t}\iint_\Gamma\mathbf{f}(\mathbf{r},t)\cdot\mathbf{g}(\mathbf{r},t)\mathrm{d}\mathbf{r}\,\mathrm{d}t. \tag{8}$$

The most important property of the Sobolev space for the stability theorem is the parameter s, which characterizes the regularity in time. More precisely, the function $(-i\omega)^s\widehat{f}(\omega)$ has to be inverse Fourier–Laplace transformable. This implies s-times continuously differentiability when s is an integer.

Other requirements for the Sobolev space are Fourier–Laplace transformability for $\sigma>0$ and a support in time of $\mathbb{R}_+$. These requirements are satisfied in common TDIE methods, because of the zero initial conditions and because only piecewise polynomials and the Dirac delta distribution will be used as test and basis functions in time.

The variational formulation of the differentiated EFIE (3) is given by

$$\forall(\dot{\mathbf{E}}^i\times\hat{\mathbf{n}})\in\mathcal{H}^{\frac{1}{2}},\ \text{search for}\ \mathbf{J}\in\mathcal{H}^{\frac{1}{2}}\ \text{such that}\ \forall\mathbf{w}\in\mathcal{H}^{-\frac{1}{2}}:$$

$$\left\langle-\hat{\mathbf{n}}\times\hat{\mathbf{n}}\times\iint_\Gamma\left(\mu\frac{\ddot{\mathbf{J}}(\mathbf{r}',\tau)}{4\pi R}-\frac{1}{\epsilon}\nabla\frac{\nabla'\cdot\mathbf{J}(\mathbf{r}',\tau)}{4\pi R}\right)\mathrm{d}\mathbf{r}',\mathbf{w}(\mathbf{r},t)\right\rangle_\sigma=\left\langle-\hat{\mathbf{n}}\times\hat{\mathbf{n}}\times\dot{\mathbf{E}}^i(\mathbf{r},t),\mathbf{w}(\mathbf{r},t)\right\rangle_\sigma. \tag{9}$$

The uniqueness and boundedness of the solution of this variational formulation will be proven in Section 3.2. Notice that if $(\mathbf{f}\times\hat{\mathbf{n}})\in\mathcal{H}^s$, then $\hat{\mathbf{n}}\times(\mathbf{f}\times\hat{\mathbf{n}})$ is an element of the dual of $\mathcal{H}^{-s}$. Furthermore, for electric current densities $\mathbf{J}\in\mathcal{H}^s$, the test space of the variational formulation is the dual of the range space of the EFIE operator [16].

2.3. Numerical discretization

The numerical discretization of the EFIE uses a triangular surface mesh on the interface Γ and discrete time levels $t_l=l\Delta t$ for $l\in\mathbb{Z}$ where Δt denotes the uniform time step size. Different discretization procedures have been used in literature. Almost all schemes can be written as a special case of the finite element method. Hence, the variational formulation (9) is used, with the electric surface current density expanded as

$$\mathbf{J}(\mathbf{r},t)=\sum_{n=1}^{N_s}\sum_{j=1}^{N_t}J_{n,j}\mathbf{h}_n(\mathbf{r})v_j(t) \tag{10}$$

in terms of N_s spatial basis functions $\mathbf{h}_n$ and N_t temporal basis functions v_j. Consequently, N_s spatial test functions $\tilde{\mathbf{h}}_m$ and N_t temporal test functions u_k are used.

The usual choice of spatial discretization in TDIE methods is a Galerkin method with Raviart–Thomas elements [21], or, equivalently, Rao–Wilton–Glisson (RWG) functions [22]. The RWG functions are linear vector functions associated with pairs of triangular facets and defined as

$$\mathbf{h}_n(\mathbf{r})=\begin{cases}\dfrac{\ell_n}{2|\Gamma_n^+|}(\mathbf{r}-\mathbf{r}_n^+), & \mathbf{r}\in\Gamma_n^+,\\ -\dfrac{\ell_n}{2|\Gamma_n^-|}(\mathbf{r}-\mathbf{r}_n^-), & \mathbf{r}\in\Gamma_n^-,\\ \mathbf{0}, & \text{elsewhere},\end{cases} \tag{11}$$

where the triangular facets Γ_n^+ and Γ_n^- share edge n of length ℓ_n, and $\mathbf{r}_n^+$ and $\mathbf{r}_n^-$ the vertices of Γ_n^+ and Γ_n^-, respectively, that are no endpoints of the shared edge. The RWG functions are element of the function space $H^{-\frac{1}{2}}(\mathrm{div},\Gamma)$ and can therefore be used in the variational formulation of the EFIE [23].

The test and basis functions in time for use in TDIE methods can be chosen according to several strategies [1,3,4]. In this paper, the MoT scheme is used, which is based on collocation and has beneficial efficiency and accuracy characteristics [11,12,24]. Hence, the test functions are given by

$$u_k(t)=\delta(t-t_k) \tag{12}$$

where δ denotes the Dirac delta distribution. The temporal basis functions are chosen as geometric translations

$$v_j(t)=T(t-j\Delta t)\quad\text{for}\ j=1,2,\ldots,N_t, \tag{13}$$

of a piecewise polynomial of degree d, i.e.,

$$T(s)=\begin{cases}a_{0d}s^d+\cdots+a_{01}s+a_{00}, & -1<\dfrac{s}{\Delta t}\le 0,\\ a_{1d}s^d+\cdots+a_{11}s+a_{10}, & 0<\dfrac{s}{\Delta t}\le 1,\\ \vdots & \vdots\\ a_{dd}s^d+\cdots+a_{d1}s+a_{d0}, & d-1<\dfrac{s}{\Delta t}\le d.\end{cases} \tag{14}$$

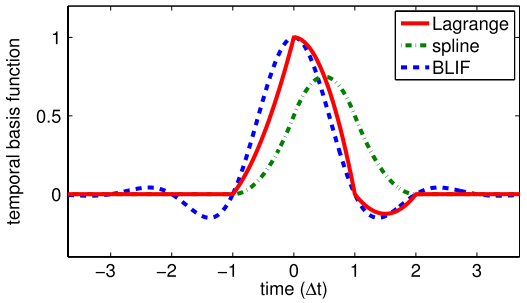

Fig. 1. Three of the most popular temporal basis functions, namely the quadratic Lagrange, quadratic spline, and bandlimited interpolation function (BLIF).

Provided d is large enough, this choice allows for the evaluation of the solution and its (anti-)derivatives in arbitrary retarded time levels, as required in TDIE methods. Furthermore, the small support of the temporal basis function results in an efficient solution procedure and causality of the discretized EFIE is achieved for arbitrary d. That is, the discretized EFIE can be written as

$$Z_0\mathbf{I}_k = \mathbf{V}_k - \sum_{j=1}^{\ell} Z_j\mathbf{I}_{k-j} \quad \text{for } k = 1, 2, \ldots, N_t \tag{15}$$

where $\mathbf{I}_k$ denotes the discrete surface current density, $\mathbf{V}_k$ the discrete incident field, and Z_j the discrete interaction matrices. The discrete solution at every time level k can be calculated from a finite range of known solutions only, resulting in an efficient marching procedure.

The choice of temporal basis function has a profound impact on numerical properties of the TDIE method, such as accuracy, efficiency, and stability [11,12]. Many different functions have been introduced in literature [25,12]. Arguably the most popular choice is the family of shifted Lagrange interpolants [13], which is depicted in Fig. 1. Other choices are spline basis functions, which have better accuracy characteristics [12], and bandlimited interpolation functions, which will not be used because they do not lead to causality of the discretized equations and thus lack the efficiency of causal basis functions [11]. In this paper, we aim to provide guidelines for the choice of temporal basis function such that the stability theorem of the Galerkin discretized EFIE can be used.

3. Stability of the variational formulation

The TDIE method for electromagnetic scattering analysis has a long history of instability. Early implementations were very hard to stabilize, even for small-scale problems. Significant progress in stabilization techniques has improved the MoT scheme such that stable results can be obtained for many different objects. However, there is no mathematical justification and stability is often obtained only after repeated computer simulations with carefully adjusted parameters. Because this is not feasible for practical purposes, it is important to use *a priori* stability analyses to design an MoT scheme with robust stability characteristics.

Analysis of the instabilities in TDIE methods is difficult due to the presence of the retarded time in the model equations. This causes a strong coupling of space and time dependencies and prevents a straightforward use of classical techniques for ordinary and delayed differential equations. Stabilization techniques have therefore been based mainly on computational experience and *a posteriori* stability analyses. Many of these algorithms do not eliminate the instability, but merely push the instability further into late-time. That is, the instability plagues the solution only when the simulation time is long compared to the time scale of the excitation. This so-called late-time instability can be deceptive and computational experiments suggest that the instability will be visible in early time when geometrically complicated scattering problems are simulated.

In this section, the stability of TDIE methods will be analyzed with a stability theorem that states uniqueness and boundedness of the solution of a specific variational formulation. A stability theorem for the original EFIE can be found in [16], which will be summarized in Section 3.1. This stability theorem will be extended to the differentiated EFIE in Section 3.2.

3.1. Stability theorem of the original EFIE

Remember that the original EFIE (1) is formulated with the electric surface current density $\mathbf{J}(\mathbf{r}, t)$ as single unknown. The EFIE could also be written with the electric surface charge density $\rho(\mathbf{r}, t)$ as additional unknown [22]. For the purpose of analyzing the equations, this can be advantageous, but for numerical discretization, it is more efficient to consider only one unknown. Since a formulation with both unknowns is used in [16], let us introduce the following Sobolev space.

Definition 5. For $s \in \mathbb{R}$ and $\sigma > 0$,

$$\mathcal{H}^s_{\rho,\mathbf{J}} = \left\{ (\rho, \mathbf{J}) \in H^s_\sigma\left(\mathbb{R}_+, H^{-\frac{1}{2}}(\Gamma)\right) \times H^s_\sigma\left(\mathbb{R}_+, TH^{-\frac{1}{2}}(\Gamma)\right),\ \nabla\cdot\mathbf{J} + \epsilon\frac{\partial\rho}{\partial t} = 0 \right\}. \tag{16}$$

The requirement $\nabla \cdot \mathbf{J} + \epsilon \frac{\partial \rho}{\partial t} = 0$ is called the continuity equation and gives a relation between the electric surface current and charge density. The Sobolev spaces (6) and (16) satisfy the following equivalence [16].

Proposition 1. $(\rho, \mathbf{J}) \in \mathcal{H}^s_{\rho,\mathbf{J}}$ *iff* $\mathbf{J} \in \mathcal{H}^s$.

Now, the original EFIE can be written as a specific variational formulation with a unique and bounded solution [16].

Theorem 2 (*Variational Formulation, [16]*). $\forall (\mathbf{E}^i \times \hat{\mathbf{n}}) \in \mathcal{H}^{\frac{3}{2}}$, *the original EFIE (1) admits the following variational formulation:*

search for $(\rho, \mathbf{J}) \in \mathcal{H}^{\frac{1}{2}}_{\rho,\mathbf{J}}$ *such that* $\forall (\widetilde{\rho}, \widetilde{\mathbf{J}}) \in \mathcal{H}^{\frac{1}{2}}_{\rho,\mathbf{J}}$:

$$b\left((\rho, \mathbf{J}), (\widetilde{\rho}, \widetilde{\mathbf{J}})\right) = \int_{\mathbb{R}} e^{-2\sigma t} \iint_{\Gamma} \left(\hat{\mathbf{n}} \times (\mathbf{E}^i \times \hat{\mathbf{n}})\right) \cdot \frac{\partial^2 \widetilde{\mathbf{J}}}{\partial t^2} \mathrm{d}\mathbf{r}\, \mathrm{d}t \tag{17}$$

with the bilinear form b defined as

$$\begin{aligned} b\left((\rho, \mathbf{J}), (\widetilde{\rho}, \widetilde{\mathbf{J}})\right) = &-\mu \int_{\mathbb{R}} e^{-2\sigma t} \iint_{\Gamma} \iint_{\Gamma} \frac{\frac{\partial}{\partial t}\mathbf{J}(\mathbf{r}', \tau)}{4\pi R} \cdot \frac{\partial^2 \widetilde{\mathbf{J}}(\mathbf{r}, t)}{\partial t^2} \mathrm{d}\mathbf{r}\, \mathrm{d}\mathbf{r}' \mathrm{d}t \\ &-\epsilon \int_{\mathbb{R}} e^{-2\sigma t} \iint_{\Gamma} \iint_{\Gamma} \frac{\rho(\mathbf{r}', \tau)}{4\pi R} \frac{\partial^3 \widetilde{\rho}(\mathbf{r}, t)}{\partial t^3} \mathrm{d}\mathbf{r}\, \mathrm{d}\mathbf{r}' \mathrm{d}t. \end{aligned} \tag{18}$$

Theorem 3 (*Uniqueness, [16]*). *If* $(\mathbf{E}^i \times \hat{\mathbf{n}}) \in \mathcal{H}^{\frac{3}{2}}$, *then the variational formulation admits a unique solution* $(\rho, \mathbf{J}) \in \mathcal{H}^{\frac{1}{2}}_{\rho,\mathbf{J}}$.

Theorem 4 (*Stability, [16]*). *The following bounds on the solution* $(\rho, \mathbf{J})$ *hold:*

$$\|\rho\|_{\frac{1}{2},\sigma,H^{-\frac{1}{2}}(\Gamma)} \leq C(\Gamma) \frac{1}{\sigma} \left\|\mathbf{E}^i \times \hat{\mathbf{n}}\right\|_{\frac{3}{2},\sigma,H^{-\frac{1}{2}}(\mathrm{div},\Gamma)}, \tag{19a}$$

$$\|\mathbf{J}\|_{\frac{1}{2},\sigma,TH^{-\frac{1}{2}}(\Gamma)} \leq C(\Gamma) \frac{1}{\sigma} \left\|\mathbf{E}^i \times \hat{\mathbf{n}}\right\|_{\frac{3}{2},\sigma,H^{-\frac{1}{2}}(\mathrm{div},\Gamma)}. \tag{19b}$$

Remember that the space–time norm (7) relates to the electromagnetic energy and stability is therefore achieved in a meaningful norm. Furthermore, the requirement $(\mathbf{E}^i \times \hat{\mathbf{n}}) \in \mathcal{H}^{\frac{3}{2}}$ of the variational formulation is usually satisfied for excitations that are chosen as a realistic representation of an electromagnetic field. That is, regularity and convergence to zero in time are obtained because the excitation is smooth for physical reasons and only excitations of finite duration will be considered.

3.2. Stability theorem of the differentiated EFIE

The stability theorem in Section 3.1 is only applicable to the original EFIE. As argued in Section 2.1, the differentiated EFIE will result in a more efficient MoT scheme than the original EFIE. Moreover, the vast majority of engineering literature on TDIE methods deals with the differentiated EFIE. Extension of the stability theorem to the differentiated EFIE is therefore important for the practical application of MoT schemes. First, let us state the stability theorem of the differentiated EFIE.

Theorem 5 (*Variational Formulation*). $\forall (\dot{\mathbf{E}}^i \times \hat{\mathbf{n}}) \in \mathcal{H}^{\frac{1}{2}}$, *the differentiated EFIE (3) admits the following variational formulation:*

search for $\mathbf{J} \in \mathcal{H}^{\frac{1}{2}}$ *such that* $\forall \mathbf{w} \in \mathcal{H}^{-\frac{1}{2}}$:

$$\left\langle \iint_{\Gamma} \left(\mu \frac{\ddot{\mathbf{J}}(\mathbf{r}', \tau)}{4\pi R} - \frac{1}{\epsilon} \nabla \frac{\nabla \cdot \mathbf{J}(\mathbf{r}, \tau)}{4\pi R} \right) \mathrm{d}\mathbf{r}', \mathbf{w} \right\rangle_{\sigma} = \left\langle \hat{\mathbf{n}} \times (\dot{\mathbf{E}}^i \times \hat{\mathbf{n}}), \mathbf{w} \right\rangle_{\sigma}. \tag{20}$$

Theorem 6 (*Uniqueness*). *If* $(\dot{\mathbf{E}}^i \times \hat{\mathbf{n}}) \in \mathcal{H}^{\frac{1}{2}}$, *then the variational formulation admits a unique solution* $\mathbf{J} \in \mathcal{H}^{\frac{1}{2}}$.

Theorem 7 (*Stability*). *The following bound on the solution* $\mathbf{J}$ *holds:*

$$\|\mathbf{J}\|_{\frac{1}{2},\sigma,-\frac{1}{2}\mathrm{div}} \leq C(\Gamma) \frac{1}{\sigma} \left\|\dot{\mathbf{E}}^i \times \hat{\mathbf{n}}\right\|_{\frac{1}{2},\sigma,-\frac{1}{2}\mathrm{div}}. \tag{21}$$

The proof of the stability theorem of the differentiated EFIE will be given subsequently. The backbone of the proof is the stability theorem of the original EFIE. More precisely, if the variational formulations of the two integral equations can be shown to be equivalent, then stability of the solution will follow.

There are two main differences between the two variational formulations. First, the electric surface charge density has been eliminated. Second, the index of the Sobolev space $\mathcal{H}^s$ has been changed for the test space. This index represents the regularity of the function space and the test functions are required to be one order of continuity higher than for the original version. This is reasonable, because using a test function that is more smooth is a natural choice in a differentiated version.

3.2.1. Elimination of the surface charge

The elimination of the electric surface charge density from the original EFIE can be performed with the continuity equation.

Lemma 8. *The bilinear form (18) is equivalent to*

$$b\left(\mathbf{J},\widetilde{\mathbf{J}}\right) = -\left\langle \iint_\Gamma \left(\mu \frac{\frac{\partial}{\partial t}\mathbf{J}(\mathbf{r}',\tau)}{4\pi R} - \frac{1}{\epsilon}\nabla \frac{\int_{-\infty}^{\tau} \nabla'_\Gamma \cdot \mathbf{J}(\mathbf{r}',\bar{t})\mathrm{d}\bar{t}}{4\pi R} \right) \mathrm{d}\mathbf{r}', \frac{\partial^2 \widetilde{\mathbf{J}}(\mathbf{r},t)}{\partial t^2} \right\rangle_\sigma \tag{22}$$

for $\mathbf{J} \in \mathcal{H}^{\frac{1}{2}}$ *and* $\widetilde{\mathbf{J}} \in \mathcal{H}^{\frac{1}{2}}$.

Proof. As stated in Theorem 2, $(\rho,\mathbf{J}) \in \mathcal{H}^{\frac{1}{2}}_{\rho,\mathbf{J}}$ and $(\widetilde{\rho},\widetilde{\mathbf{J}}) \in \mathcal{H}^{\frac{1}{2}}_{\rho,\mathbf{J}}$ for the bilinear form (18). This yields $\mathbf{J} \in \mathcal{H}^{\frac{1}{2}}$ and $\widetilde{\mathbf{J}} \in \mathcal{H}^{\frac{1}{2}}$ by Proposition 1. Furthermore, the continuity equation $\nabla \cdot \mathbf{J} + \epsilon \frac{\partial \rho}{\partial t} = 0$ holds, which can be rewritten into $\rho(\mathbf{r},t) = -\frac{1}{\epsilon}\int_{-\infty}^{t} \nabla \cdot \mathbf{J}(\mathbf{r},\bar{t})\mathrm{d}\bar{t}$. Substitution of this expression of the surface charge into the bilinear form (18) results in

$$\begin{aligned} b\left(\mathbf{J},\widetilde{\mathbf{J}}\right) &= -\mu \left\langle \iint_\Gamma \frac{\frac{\partial}{\partial t}\mathbf{J}(\mathbf{r}',\tau)}{4\pi R}\mathrm{d}\mathbf{r}', \frac{\partial^2 \widetilde{\mathbf{J}}(\mathbf{r},t)}{\partial t^2} \right\rangle_\sigma - \frac{1}{\epsilon}\left\langle \iint_\Gamma \frac{\int_{-\infty}^{\tau} \nabla'_\Gamma \cdot \mathbf{J}(\mathbf{r}',\bar{t})\mathrm{d}\bar{t}}{4\pi R}\mathrm{d}\mathbf{r}', \frac{\partial^2}{\partial t^2}\left(\nabla \cdot \widetilde{\mathbf{J}}(\mathbf{r},t)\right) \right\rangle_\sigma \\ &= -\mu \left\langle \iint_\Gamma \frac{\frac{\partial}{\partial t}\mathbf{J}(\mathbf{r}',\tau)}{4\pi R}\mathrm{d}\mathbf{r}', \frac{\partial^2 \widetilde{\mathbf{J}}(\mathbf{r},t)}{\partial t^2} \right\rangle_\sigma - \frac{1}{\epsilon}\left\langle \iint_\Gamma \frac{\int_{-\infty}^{\tau} \nabla'_\Gamma \cdot \mathbf{J}(\mathbf{r}',\bar{t})\mathrm{d}\bar{t}}{4\pi R}\mathrm{d}\mathbf{r}', \nabla \cdot \frac{\partial^2 \widetilde{\mathbf{J}}(\mathbf{r},t)}{\partial t^2} \right\rangle_\sigma \end{aligned}$$

where the second equality holds because the interface is stationary: $\frac{\partial}{\partial t}\Gamma = 0$. To perform integration by parts on the interface Γ, let us use $\nabla \cdot (\psi \mathbf{a}) = (\nabla\psi)\cdot\mathbf{a} + \psi\nabla\cdot\mathbf{a}$ and Stokes' theorem, that is, $\iint_\Gamma \nabla \cdot \mathbf{a}\mathrm{d}A = \int_{\partial\Gamma} \vec{\nu}\cdot\mathbf{a}\mathrm{d}s$ for arbitrary $\mathbf{a} \in \mathcal{H}^s$, where $\vec{\nu}$ denotes the vector that is normal to both Γ and $\hat{\mathbf{n}}$. Notice that when Γ is closed, no $\vec{\nu}$ exists and the boundary terms is zero. Otherwise, integration by parts results in

$$\begin{aligned} b\left(\mathbf{J},\widetilde{\mathbf{J}}\right) = -\mu \left\langle \iint_\Gamma \frac{\frac{\partial}{\partial t}\mathbf{J}(\mathbf{r}',\tau)}{4\pi R}\mathrm{d}\mathbf{r}', \frac{\partial^2 \widetilde{\mathbf{J}}(\mathbf{r},t)}{\partial t^2} \right\rangle_\sigma + \frac{1}{\epsilon}\left\langle \nabla \iint_\Gamma \frac{\int_{-\infty}^{\tau} \nabla'_\Gamma \cdot \mathbf{J}(\mathbf{r}',\bar{t})\mathrm{d}\bar{t}}{4\pi R}\mathrm{d}\mathbf{r}', \frac{\partial^2 \widetilde{\mathbf{J}}(\mathbf{r},t)}{\partial t^2} \right\rangle_\sigma \\ - \int_{\partial\Gamma} \vec{\nu}\cdot\left(\iint_\Gamma \frac{\int_{-\infty}^{\tau} \nabla'_\Gamma \cdot \mathbf{J}(\mathbf{r}',\bar{t})\mathrm{d}\bar{t}}{4\pi R}\mathrm{d}\mathbf{r}' \frac{\partial^2 \widetilde{\mathbf{J}}(\mathbf{r},t)}{\partial t^2} \right)\mathrm{d}s. \end{aligned}$$

Because $\widetilde{\mathbf{J}} \in \mathcal{H}^{\frac{1}{2}}$, we have $\widetilde{\mathbf{J}} \in H^{-\frac{1}{2}}_{\mathrm{div}}(\Gamma)$ for all $t \in \mathbb{R}$. A characteristic of this function space is that the normal component on the boundary is zero, that is, $\vec{\nu}(\mathbf{r})\cdot\widetilde{\mathbf{J}}(\mathbf{r},t) = 0$ for all $t \in \mathbb{R}$. This yields that the boundary term is zero and the bilinear form (22) is obtained. □

3.2.2. Integration by parts

To obtain concise equations, let us abbreviate the original and differentiated EFIE as $\hat{\mathbf{n}}\times(\mathbf{E}^i\times\hat{\mathbf{n}}) = \mathcal{E}(\mathbf{J})$ and $\hat{\mathbf{n}}\times(\dot{\mathbf{E}}^i\times\hat{\mathbf{n}}) = \dot{\mathcal{E}}(\mathbf{J})$, respectively. Notice that the difference between the two versions of the EFIE is only a time derivative, that is, $\dot{\mathcal{E}} = \frac{\partial}{\partial t}\mathcal{E}$. Hence, integration by parts will be used, but remember that the inner product (8) uses a time-dependent weight.

Lemma 9. *If*

$$\mathbf{v} = 2\sigma\mathbf{w} - \frac{\partial \mathbf{w}}{\partial t} \tag{23}$$

then

$$\mathbf{v} \in \mathcal{H}^{-\frac{3}{2}} \iff \mathbf{w} \in \mathcal{H}^{-\frac{1}{2}}.$$

Proof. Most of the properties of the Sobolev space $\mathcal{H}^s$ are expressed in the Fourier–Laplace domain, that is, $\widehat{f}(\omega) = \int_{-\infty}^{\infty} e^{i\omega t} f(t)\mathrm{d}t$ for $\omega = \eta + i\sigma$ and $\sigma > 0$, as given by Definition 2. To this end, the equation $\mathbf{v} = 2\sigma\mathbf{w} - \frac{\partial \mathbf{w}}{\partial t}$ is written as

$$\widehat{\mathbf{v}} = 2\sigma\widehat{\mathbf{w}} - (-i\omega\widehat{\mathbf{w}}) = (2\sigma + i\omega)\widehat{\mathbf{w}} = (\sigma + i\eta)\widehat{\mathbf{w}} = i(\eta - i\sigma)\widehat{\mathbf{w}} = i\bar{\omega}\widehat{\mathbf{w}} \tag{24}$$

where $\bar{\omega}$ denotes the complex conjugate of ω. Because $\mathbf{f} \in \mathcal{H}^s$ if its norm $\|\mathbf{f}\|_{\sigma,s,-\frac{1}{2}\mathrm{div}}$ is bounded, let us consider the norm of $\mathbf{v}$, that is,

$$\begin{aligned}
\|\mathbf{v}\|^2_{\sigma,s,-\frac{1}{2}\mathrm{div}} &= \frac{1}{2\pi}\int_{-\infty+i\sigma}^{+\infty+i\sigma} |\omega|^{2s}\, \|\widehat{\mathbf{v}}(\cdot,\omega)\|^2_{H^{-\frac{1}{2}}(\mathrm{div},\Gamma)}\, \mathrm{d}\omega \\
&= \frac{1}{2\pi}\int_{-\infty+i\sigma}^{+\infty+i\sigma} |\omega|^{2s}\, |i\bar{\omega}|^2\, \|\widehat{\mathbf{w}}(\cdot,\omega)\|^2_{H^{-\frac{1}{2}}(\mathrm{div},\Gamma)}\, \mathrm{d}\omega \\
&= \frac{1}{2\pi}\int_{-\infty+i\sigma}^{+\infty+i\sigma} |\omega|^{2(s+1)}\, \|\widehat{\mathbf{w}}(\cdot,\omega)\|^2_{H^{-\frac{1}{2}}(\mathrm{div},\Gamma)}\, \mathrm{d}\omega \\
&= \|\mathbf{w}\|^2_{\sigma,s+1,-\frac{1}{2}\mathrm{div}}. \qquad (25)
\end{aligned}$$

Hence, $\mathbf{v} \in \mathcal{H}^{-\frac{3}{2}} \iff \mathbf{w} \in \mathcal{H}^{-\frac{1}{2}}$. □

Lemma 10. *For* $(\mathbf{E}^i \times \hat{\mathbf{n}}) \in \mathcal{H}^{\frac{3}{2}}$, $\mathbf{J} \in \mathcal{H}^{\frac{1}{2}}$ *and* $\mathbf{w} \in \mathcal{H}^{-\frac{1}{2}}$,

$$\left\langle \dot{\mathcal{E}}(\mathbf{J}), \mathbf{w} \right\rangle_\sigma = \left\langle \mathcal{E}(\mathbf{J}), 2\sigma\mathbf{w} - \frac{\partial \mathbf{w}}{\partial t} \right\rangle_\sigma, \qquad (26)$$

$$\left\langle \hat{\mathbf{n}} \times (\dot{\mathbf{E}}^i \times \hat{\mathbf{n}}), \mathbf{w} \right\rangle_\sigma = \left\langle \hat{\mathbf{n}} \times (\mathbf{E}^i \times \hat{\mathbf{n}}), 2\sigma\mathbf{w} - \frac{\partial \mathbf{w}}{\partial t} \right\rangle_\sigma. \qquad (27)$$

Proof. By definition of the original and differential EFIE, $\dot{\mathcal{E}}(\mathbf{J}) = \frac{\partial}{\partial t}\mathcal{E}(\mathbf{J})$. Then, integration by parts results in

$$\begin{aligned}
\left\langle \dot{\mathcal{E}}(\mathbf{J}), \mathbf{w} \right\rangle_\sigma &= \iint_\Gamma \int_{-\infty}^{+\infty} e^{-2\sigma t}\, \frac{\partial \mathcal{E}(\mathbf{J})}{\partial t} \cdot \mathbf{w} \mathrm{d}t\, \mathrm{d}\mathbf{r} \\
&= \iint_\Gamma \left(\left[e^{-2\sigma t}\, \mathcal{E}(\mathbf{J}) \cdot \mathbf{w} \right]_{t=-\infty}^{+\infty} - \int_{-\infty}^{+\infty} \mathcal{E}(\mathbf{J}) \cdot \frac{\partial \left(e^{-2\sigma t}\, \mathbf{w} \right)}{\partial t} \mathrm{d}t \right) \mathrm{d}\mathbf{r} \\
&= \int_{-\infty}^{+\infty} e^{-2\sigma t} \iint_\Gamma \left(2\sigma\, \mathcal{E}(\mathbf{J}) \cdot \mathbf{w} - \mathcal{E}(\mathbf{J}) \cdot \frac{\partial \mathbf{w}}{\partial t} \right) \mathrm{d}\mathbf{r}\, \mathrm{d}t \\
&= \left\langle \mathcal{E}(\mathbf{J}), 2\sigma\mathbf{w} - \frac{\partial \mathbf{w}}{\partial t} \right\rangle_\sigma \qquad (28)
\end{aligned}$$

where the boundary term is zero because $\mathbf{w} \in \mathcal{H}^{-\frac{1}{2}}$, so $\mathbf{w} = 0$ for $t < 0$ and $t \to \infty$. Changing $\dot{\mathcal{E}}(\mathbf{J})$ by $\hat{\mathbf{n}} \times (\dot{\mathbf{E}}^i \times \hat{\mathbf{n}})$ in Eq. (28) proves the second part of the lemma. □

3.2.3. Equivalent variational formulations

Now, one can use the previous lemmas to prove the equivalence between the variational formulation of the original and differentiated EFIE.

Theorem 11. *The variational formulation (17) of the original EFIE and variational formulation (9) of the differentiated EFIE are equivalent.*

Proof. Let us start with the variational formulation (9) of the differentiated EFIE and proceed to the variational formulation (17) of the original EFIE. With $\mathcal{E}$ and $\dot{\mathcal{E}}$ denoting the original and differentiated EFIE operators, respectively, the variational formulation of the differentiated EFIE reads:

search for $\mathbf{J} \in \mathcal{H}^{\frac{1}{2}}$ such that $\forall \mathbf{w} \in \mathcal{H}^{-\frac{1}{2}}$:
$\left\langle \dot{\mathcal{E}}(\mathbf{J}), \mathbf{w} \right\rangle_\sigma = \left\langle \hat{\mathbf{n}} \times (\dot{\mathbf{E}}^i \times \hat{\mathbf{n}}), \mathbf{w} \right\rangle_\sigma$.

With Lemma 10, this is equivalent to:

search for $\mathbf{J} \in \mathcal{H}^{\frac{1}{2}}$ such that $\forall \mathbf{w} \in \mathcal{H}^{-\frac{1}{2}}$:
$\left\langle \mathcal{E}(\mathbf{J}), 2\sigma\mathbf{w} - \frac{\partial \mathbf{w}}{\partial t} \right\rangle_\sigma = \left\langle \hat{\mathbf{n}} \times (\mathbf{E}^i \times \hat{\mathbf{n}}), 2\sigma\mathbf{w} - \frac{\partial \mathbf{w}}{\partial t} \right\rangle_\sigma$.

With Lemma 9, this is equivalent to:

search for $\mathbf{J} \in \mathcal{H}^{\frac{1}{2}}$ such that $\forall \mathbf{v} \in \mathcal{H}^{-\frac{3}{2}}$:
$\langle \mathcal{E}(\mathbf{J}), \mathbf{v} \rangle_\sigma = \left\langle \hat{\mathbf{n}} \times (\mathbf{E}^i \times \hat{\mathbf{n}}), \mathbf{v} \right\rangle_\sigma$.

Notice that this variational formulation is written in a Petrov–Galerkin form, where the test and solution spaces are defined differently. On the contrary, the variational formulation (17) of the original EFIE uses equivalent test and solution spaces and is thus written in a Galerkin form. The property $\mathbf{f} \in \mathcal{H}^s \iff \frac{\partial^2 \mathbf{f}}{\partial t^2} \in \mathcal{H}^{s+2}$ of Sobolev spaces yields an equivalence between testing with $\mathbf{v}$ and $\frac{\partial^2 \widetilde{\mathbf{J}}}{\partial t^2}$, where $\mathbf{v} \in \mathcal{H}^{-\frac{3}{2}}$ and $\widetilde{\mathbf{J}} \in \mathcal{H}^{\frac{1}{2}}$. Thus, the variational formulation is equivalent to:

$$\text{search for } \mathbf{J} \in \mathcal{H}^{\frac{1}{2}} \text{ such that } \forall \widetilde{\mathbf{J}} \in \mathcal{H}^{\frac{1}{2}} : \quad \left\langle \mathcal{E}(\mathbf{J}), \frac{\partial^2 \widetilde{\mathbf{J}}}{\partial t^2} \right\rangle_\sigma = \left\langle \hat{\mathbf{n}} \times (\mathbf{E}^i \times \hat{\mathbf{n}}), \frac{\partial^2 \widetilde{\mathbf{J}}}{\partial t^2} \right\rangle_\sigma .$$

With Lemma 8, we have $\left\langle \mathcal{E}(\mathbf{J}), \frac{\partial^2 \widetilde{\mathbf{J}}}{\partial t^2} \right\rangle_\sigma = b(\mathbf{J}, \widetilde{\mathbf{J}})$ and the variational formulation of the original EFIE is obtained. □

This theorem states that the variational formulations of the original and differentiated EFIE are equivalent. Because the solution of the original EFIE is unique and bounded, this holds for the differentiated EFIE as well, which completes the stability proof for the differentiated EFIE.

4. Stability of Petrov–Galerkin schemes

As explained in Section 3.1, the variational formulation of the original EFIE admits a unique and bounded solution $\mathbf{J} \in \mathcal{H}^{\frac{1}{2}}$. This stability theorem has been extended to the differentiated EFIE in Section 3.2, where the testing space is given by $\mathcal{H}^{-\frac{1}{2}}$ instead of $\mathcal{H}^{-\frac{3}{2}}$ for the original EFIE. In this section, the EFIE will be discretized in time with a Petrov–Galerkin scheme where test and basis functions are chosen as element of these Sobolev spaces.

Notice that the stability theorems of the EFIE in Section 3 concern the continuous equations. To the best of the author's knowledge, no stability theorem for the discretized EFIE has been given in literature and proving this is outside the scope of this paper. Nonetheless, the presented stability theorem is important for the choice of test and basis functions, as will be confirmed by the computational experiments in Section 5. Furthermore, an inner product (8) with zero weight will be used in the numerical discretization, that is $\sigma = 0$. In the stability theorem, an arbitrary $\sigma > 0$ is required, which makes this choice invalid. However, the discrete equations become considerably more efficient to solve for $\sigma = 0$ and this will be used nevertheless. This choice has been justified in [14].

4.1. Discretely equivalent Petrov–Galerkin schemes

Remember that the parameter s of the Sobolev space $\mathcal{H}^s$ characterizes the regularity in time. Consequently, the Dirac delta distribution is not an element of the testing space for the differentiated EFIE, which prohibits the use of the MoT scheme. Nonetheless, for carefully chosen temporal basis functions, the stability theorem can be used for the MoT scheme. This will be proven with the aid of discretely equivalent Petrov–Galerkin schemes that fit within the functional framework of the stability theorem.

Definition 6. The MoT scheme and Petrov–Galerkin scheme are discretely equivalent if $Z_j^{\mathrm{MoT}} = Z_j^{\mathrm{P-G}}$ for $j = 1, 2, \ldots, \ell$.

An important corollary of the fact that both schemes are discretely equivalent is that both schemes share the same stability characteristics, because stability is independent of the excitation. In particular, for a Petrov–Galerkin scheme that fits within the stability theorem, an MoT scheme could be derived that is discretely equivalent and therefore stable as well. To obtain concise equations, discrete equivalence of the numerical schemes can be simplified to equivalence of an arbitrary matrix element.

Lemma 12. *If*

$$\int_{\mathbb{R}} \left(\frac{\mathrm{d}^\alpha}{\mathrm{d}t^\alpha} T_j(\tau) \right) \delta(t - t_k) \mathrm{d}t = \int_{\mathbb{R}} \left(\frac{\mathrm{d}^\alpha}{\mathrm{d}t^\alpha} u_j(\tau) \right) v_k(t) \mathrm{d}t \quad \text{for } \alpha \in \{-1, 0, 1, 2\} \tag{29}$$

then the MoT scheme with temporal basis functions T_j and Petrov–Galerkin scheme with basis and test and functions u_j and v_k, respectively, are discretely equivalent for the EFIE.

Proof. For an arbitrary $j, k \in \{1, 2, \ldots, N_t\}$ and $m, n \in \{1, 2, \ldots, N_s\}$, the element $(Z_i)_{mn}$ with $i = k - j$ is given by

$$\begin{aligned} (Z_j^{\mathrm{MoT}})_{mn} &= \left\langle \mathcal{E}\left(\mathbf{f}_n(\mathbf{r}') T_j(\tau)\right), \mathbf{f}_m(\mathbf{r}) \delta(t - t_k) \right\rangle \\ &= \iint_\Gamma \iint_\Gamma \left(\mu \frac{\mathbf{f}_n(\mathbf{r}') \int_{\mathbb{R}} \dot{T}_j(\tau) \delta(t - t_k) \mathrm{d}t}{4\pi R} - \frac{1}{\epsilon} \nabla \frac{\nabla' \cdot \mathbf{f}_n(\mathbf{r}') \int_{\mathbb{R}} \int_{-\infty}^{\tau} T_j(\bar{t}) \mathrm{d}\bar{t}\, \delta(t - t_k) \mathrm{d}t}{4\pi R} \right) \mathrm{d}\mathbf{r}' \cdot \mathbf{f}_m(\mathbf{r}) \mathrm{d}\mathbf{r}, \end{aligned}$$

$$
\begin{aligned}
(Z_j^{\mathrm{P-G}})_{mn} &= \left\langle \mathcal{E}\left(\mathbf{f}_n(\mathbf{r}')u_j(\tau)\right), \mathbf{f}_m(\mathbf{r})v_k(t)\right\rangle \\
&= \iint_\Gamma \iint_\Gamma \left(\mu \frac{\mathbf{f}_n(\mathbf{r}') \int_{\mathbb{R}} \dot{u}_j(\tau) v_k(t) \mathrm{d}t}{4\pi R} - \frac{1}{\epsilon} \nabla \frac{\nabla' \cdot \mathbf{f}_n(\mathbf{r}') \int_{\mathbb{R}} \int_{-\infty}^{\tau} u_j(\bar{t}) \mathrm{d}\bar{t}\, v_k(t) \mathrm{d}t}{4\pi R} \right) \mathrm{d}\mathbf{r}' \cdot \mathbf{f}_{m(\mathbf{r})} \mathrm{d}\mathbf{r}
\end{aligned}
$$

for the original EFIE. Hence, if

$$
\begin{aligned}
\int_{\mathbb{R}} \dot{T}_j(\tau)\delta(t-t_k)\mathrm{d}t &= \int_{\mathbb{R}} \dot{u}_j(\tau) v_k(t) \mathrm{d}t, \\
\int_{\mathbb{R}} \int_{-\infty}^{\tau} T_j(\bar{t})\mathrm{d}\bar{t}\, \delta(t-t_k)\mathrm{d}t &= \int_{\mathbb{R}} \int_{-\infty}^{\tau} u_j(\bar{t})\mathrm{d}\bar{t}\, v_k(t)\mathrm{d}t,
\end{aligned}
$$

then $(Z_j^{\mathrm{MoT}})_{mn} = (Z_j^{\mathrm{P-G}})_{mn}$. For the differentiated EFIE a similar condition can be proven analogously, but now with the basis function and its second derivative. Consequently, if $\left\langle \frac{\mathrm{d}^\alpha}{\mathrm{d}t^\alpha} T_j(\tau), \delta(t-t_k) \right\rangle = \left\langle \frac{\mathrm{d}^\alpha}{\mathrm{d}t^\alpha} u_j(\tau), v_k(t) \right\rangle$ for $\alpha \in \{-1, 0, 1, 2\}$ then the MoT scheme and Petrov–Galerkin scheme are discretely equivalent for both the original and differentiated EFIE. □

Notice that this lemma involves three sets of functions, i.e., T_j, u_j and v_k. In next sections, this lemma will be used to design numerical schemes by computing one of these sets of functions given the other two sets. In particular, for a given Petrov–Galerkin scheme with a set of basis and test functions u_j and v_k, respectively, design a MoT scheme with basis functions T_j.

Theorem 13 (*Discretely Equivalent Schemes*)**.** *A Petrov–Galerkin scheme with basis and test functions denoted by $u(t)$ and $v(t)$, respectively, and a MoT scheme with basis function denoted by $T(t)$ are discretely equivalent if*

$$
T(t) = \int_{-\infty}^{\infty} u(s+t)v(s)\mathrm{d}s \tag{30}
$$

and u and T two times continuously differentiable.

Proof. The two schemes are discretely equivalent if the requirement (29) holds. Remember that we have $u_j(t) = u(t-t_j)$ and similar for the other test and basis functions. Furthermore, $\tau = t - R/c$ with $R \geq 0$ arbitrary. Then,

$$
\begin{aligned}
\int_{\mathbb{R}} \left(\frac{\mathrm{d}^n}{\mathrm{d}t^n} T_j(\tau) \right) \delta_k(t) \mathrm{d}t &= \int_{-\infty}^{\infty} \left(\frac{\mathrm{d}^n}{\mathrm{d}t^n} T(\tau - t_j) \right) \delta(t-t_k)\mathrm{d}t \\
&= T^{(n)}(\tau_{k-j}) \\
&= \int_{-\infty}^{\infty} u^{(n)}(s+\tau_{k-j}) v(s) \mathrm{d}s \\
&= \int_{-\infty}^{\infty} \left(\frac{\mathrm{d}^n}{\mathrm{d}t^n} u(\tau - t_j) \right) v(t-t_k)\mathrm{d}t \\
&= \int_{\mathbb{R}} \left(\frac{\mathrm{d}^n}{\mathrm{d}t^n} u_j(\tau) \right) v_k(t) \mathrm{d}t
\end{aligned}
$$

for all $n \leq 2$, where a change of variables $s = t - t_k$ has been used and where $\tau_{k-j} = t_{k-j} - \frac{R}{c}$. □

An important remark is that the continuity requirements in Theorem 13 can be alleviated for the EFIE, using similar techniques as in [26]. The main argument is that since the retarded potentials intertwine space and time, the regularizing surface integrals can be used to prove discrete equivalency even for Dirac delta distributions as test space.

4.2. Equivalence for the lowest order stable Petrov–Galerkin scheme

The aim of this paper is to design a stable MoT scheme for the differentiated EFIE. To this end, let us consider the Petrov–Galerkin scheme with test and basis functions that fits within the functional framework and design a discretely equivalent MoT scheme. The test and solution spaces are given by $\mathcal{H}^{-\frac{1}{2}}$ and $\mathcal{H}^{\frac{1}{2}}$, respectively. Let us consider the lowest order piecewise polynomials that fit within these Sobolev spaces. That is, let us use the step function $v_k^{\mathrm{step}}(t) = v^{\mathrm{step}}(t-t_k)$, given by

$$
v^{\mathrm{step}}(t) = \begin{cases} \dfrac{1}{\Delta t}, & -\Delta t < t \leq 0, \\ 0, & \text{else}, \end{cases} \tag{31}
$$

as test function and as basis function $u_j^{\text{hat}}(t) = u^{\text{hat}}(t - t_j)$ the hat function, given by

$$u^{\text{hat}}(t) = \begin{cases} 1 - \dfrac{|t|}{\Delta t}, & |t| \leq \Delta t, \\ 0, & \text{else.} \end{cases} \tag{32}$$

For this choice of Petrov–Galerkin scheme, a temporal basis function for a discretely equivalent MoT scheme can be designed as a corollary of Theorem 13.

Corollary 14. *The differentiated EFIE discretized with the Petrov–Galerkin scheme with step test functions and hat basis functions is discretely equivalent to the MoT scheme with quadratic spline basis functions, given by*

$$T^{\text{qs}}(t) = \begin{cases} \dfrac{1}{2}\left(\dfrac{t}{\Delta t}\right)^2 + \dfrac{t}{\Delta t} + \dfrac{1}{2} & -\Delta t < t \leq 0, \\ -\left(\dfrac{t}{\Delta t}\right)^2 + \dfrac{t}{\Delta t} + \dfrac{1}{2} & 0 < t \leq \Delta t, \\ \dfrac{1}{2}\left(\dfrac{t}{\Delta t}\right)^2 - 2\dfrac{t}{\Delta t} + 2 & \Delta t < t \leq 2\Delta t, \\ 0 & \textit{else}. \end{cases} \tag{33}$$

Proof. Substitution of the step test functions and hat basis functions into expression (30) of the MoT basis function yields

$$\int_{-\infty}^{\infty} u^{\text{hat}}(s+t)v^{\text{step}}(s)\mathrm{d}s = \begin{cases} \dfrac{1}{2}\dfrac{t^2}{\Delta t^2} + \dfrac{t}{\Delta t} + \dfrac{1}{2}, & -\Delta t < t \leq 0, \\ -\dfrac{t^2}{\Delta t^2} + \dfrac{t}{\Delta t} + \dfrac{1}{2}, & 0 < t \leq \Delta t, \\ \dfrac{1}{2}\dfrac{t^2}{\Delta t^2} - 2\dfrac{t}{\Delta t} + 2, & \Delta t < t \leq 2\Delta t \end{cases} \tag{34}$$

with straightforward calculus. □

4.3. Equivalence for the quadratic Lagrange MoT scheme

For a given Petrov–Galerkin scheme, a discretely equivalent MoT scheme has been derived in the previous section. Here, the reverse will be performed. In particular, a discretely equivalent Petrov–Galerkin scheme for a MoT scheme with the broadly used quadratic Lagrange basis functions [27], defined as

$$T^{\text{qL}}(t) = \begin{cases} \dfrac{1}{2}\left(\dfrac{t}{\Delta t}\right)^2 + \dfrac{3}{2}\dfrac{t}{\Delta t} + 1 & -\Delta t < t \leq 0, \\ -\left(\dfrac{t}{\Delta t}\right)^2 + 1 & 0 < t \leq \Delta t, \\ \dfrac{1}{2}\left(\dfrac{t}{\Delta t}\right)^2 - \dfrac{3}{2}\dfrac{t}{\Delta t} + 1 & \Delta t < t \leq 2\Delta t, \\ 0 & \text{else}, \end{cases} \tag{35}$$

will be given. However, two unknowns are present in the Petrov–Galerkin scheme, namely the test and basis function. To obtain a unique, discretely equivalent Petrov–Galerkin scheme, either the test or basis function has to be chosen in advance. Here, step test functions will be chosen, because these are the lowest-order test functions that fit within the functional framework of the stability theorem.

Corollary 15. *The differentiated EFIE discretized with the MoT scheme with quadratic Lagrange basis functions is discretely equivalent to the Petrov–Galerkin scheme with step test functions and shifted hat basis functions, given by*

$$u^{\text{shiftedhat}}(t) = \begin{cases} \dfrac{t}{\Delta t} + \dfrac{3}{2}, & -\Delta t < t \leq 0, \\ -\dfrac{t}{\Delta t} + \dfrac{1}{2}, & 0 < t \leq \Delta t, \\ 0, & \textit{else}. \end{cases} \tag{36}$$

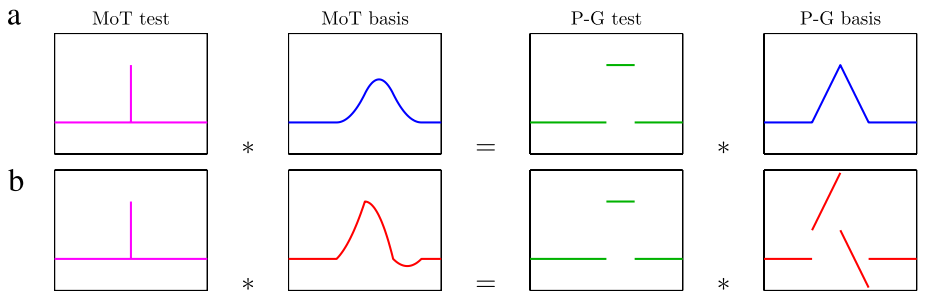

Fig. 2. Equivalence between the MoT and Petrov–Galerkin scheme for (a) quadratic spline basis functions (33) and (b) quadratic Lagrange basis functions (35).

Proof. Given the functions $T(t)$ and $v(t)$, Eq. (30) can be solved for $u(t)$ with straightforward calculus. However, for brevity, it is easier to check if the Petrov–Galerkin scheme with step test functions and shifted hat basis functions results in the quadratic Lagrange basis functions. Indeed, substitution of (36) and (31) into (30) immediately results in (35). □

The shifted hat function is discontinuous and thus not an element of $\mathscr{H}^{\frac{1}{2}}$. Hence, the basis function does not fit within the functional framework and the stability theorem can therefore not be used for the MoT scheme with quadratic Lagrange basis functions.

4.4. Summary

In this section, two discretely equivalent MoT and Petrov–Galerkin schemes have been designed. First, the Petrov–Galerkin scheme with step test functions and hat basis functions fits within the functional framework and is discretely equivalent with an MoT scheme with quadratic spline basis functions. Second, the MoT scheme with quadratic Lagrange basis functions is discretely equivalent with a Petrov–Galerkin scheme with step test functions and shifted hat basis functions. This is depicted in Fig. 2 and leads to the conclusion that the stability theorem can be used for the MoT scheme with quadratic spline basis functions, but not for quadratic Lagrange basis functions.

5. Computational experiments

The stability analysis in this paper suggests that the differentiated EFIE discretized with the MoT scheme employing quadratic spline basis functions is unconditionally stable. This cannot be proven for quadratic Lagrange basis functions with the presented stability analysis. In this section, computational experiments confirm the stability characteristics. In particular, all simulations performed with the quadratic spline basis functions are stable. It should be noted that stable simulations could only be achieved with the use of quasi-exact integration [13].

Let us consider a sphere of radius 1 m with a triangular surface mesh consisting of 356 edges. The time step size is chosen as $\Delta t = 10^{-9}$ s. The outer surface integral is approximated with a Gaussian quadrature with 73 points, whereas the inner integral is computed with analytic expressions. The MoT scheme has been applied to the differentiated EFIE with quadratic Lagrange and spline basis functions. The electric surface current density at the top of the sphere, depicted in Fig. 3, clearly shows an alternating, exponentially increasing solution for the quadratic Lagrange basis function. The use of quadratic spline basis functions results in a stable MoT scheme, as verified by the polynomial spectrum that resides within the unit disk of the complex plane [10].

In the second computer simulation, the scattering by a generic aircraft geometry with a size of 60 m is being analyzed. The surface mesh consists of 6756 edges and is depicted in Fig. 4(a). The time step size is chosen as 0.6 lm. Again, the MoT scheme for the differentiated EFIE is used where the outer surface integral is approximated with a Gaussian quadrature with 73 points and the inner integral computed analytically. As incident wave field, a modulated Gaussian plane wave is used with center frequency 16.7 MHz and bandwidth 8.3 MHz. Fig. 5 depicts the electric surface current density at the tail tip. The quadratic Lagrange basis function clearly results in an unstable computer simulation, whereas the quadratic spline basis functions remain stable for the entire simulation time of 10 000 discrete time levels. Furthermore, the scattered electric field has been calculated for the aircraft excited by a sinusoidal wave field with a wavelength of 6 m. The magnitude of the incident and scattered electric field intensity has been calculated on a horizontal plane through the aircraft and is depicted in Fig. 4(b).

The computational experiments confirm that the choice of the temporal basis function has a profound impact on the stability of the MoT scheme. In particular, quadratic spline basis functions fit within the stability theorem and result in stable simulations. The quadratic Lagrange basis functions on the other hand do not satisfy all requirements of the stability theorem and unstable simulations are obtained. The numerical stability of the quadratic spline basis function has been confirmed experimentally on both the academic test case of a sphere and the simulation on a realistic aircraft. More stable computer simulations of the MoT scheme with quadratic spline basis functions can be found in [28].

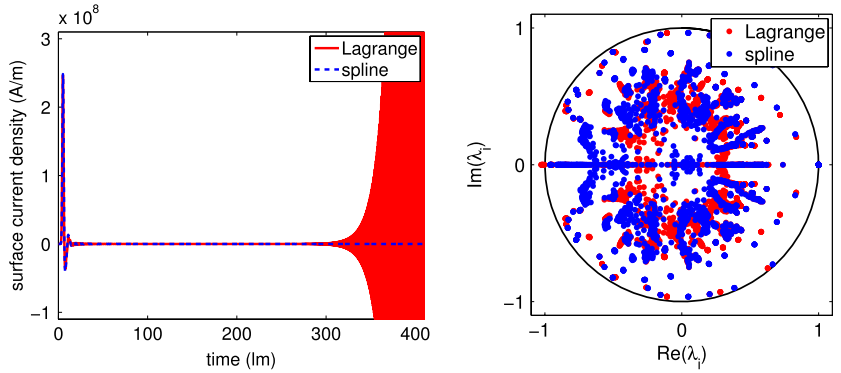

(a) Discrete electric surface current density. (b) Polynomial eigenvalues.

Fig. 3. Discrete solution on a sphere with quadratic basis functions.

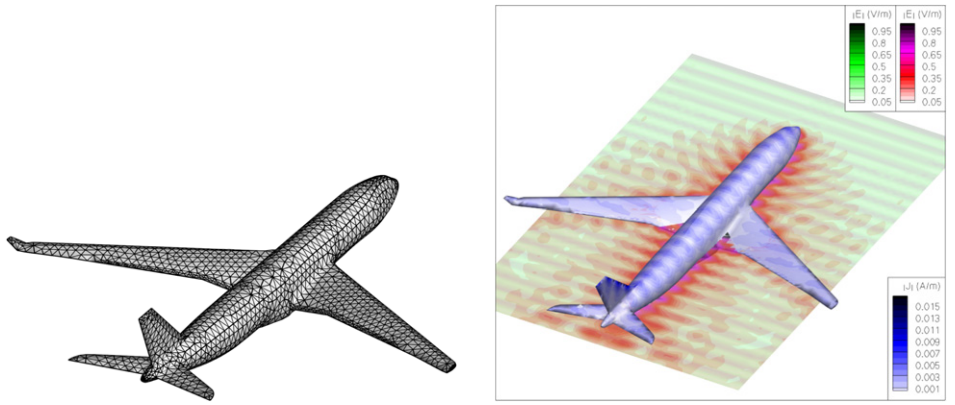

(a) Surface mesh. (b) Magnitude of the incident electric field intensity (green), electric surface current density (blue) and scattered electric field intensity (red).

Fig. 4. Simulation on a generic aircraft. (For interpretation of the references to color in this figure legend, the reader is referred to the web version of this article.)

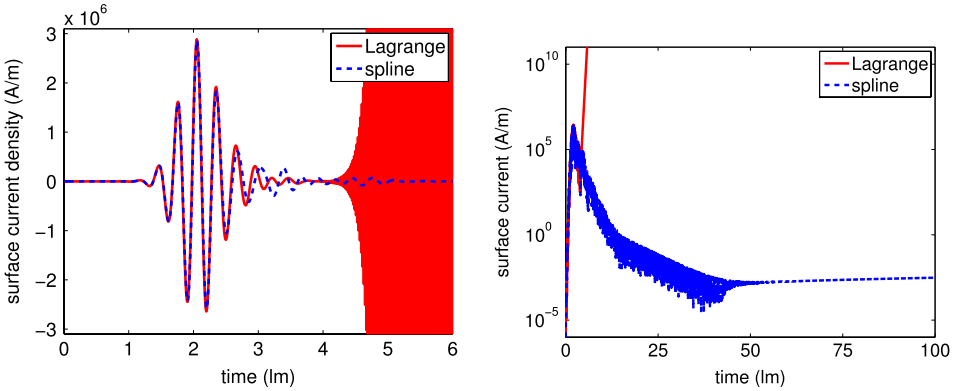

(a) Linear scale. (b) Logarithmic scale.

Fig. 5. Discrete electric surface current density on the tail tip of a generic aircraft with quadratic basis functions.

6. Conclusions

The MoT scheme with the differentiated EFIE is the most efficient and popular TDIE method for electromagnetics. Its stability has been analyzed starting from a functional framework and stability theorem of a variational formulation of the original EFIE. This stability theorem has been extended to the differentiated EFIE, for which another test space is required. On

a discrete level, a space–time Petrov–Galerkin method that fits within the functional framework has been used. A discretely equivalent collocation scheme motivates the choice of quadratic spline basis functions. Computational experiments for an aircraft confirm the stability of this particular TDIE method for electromagnetics.

References

[1] B. Shanker, A.A. Ergin, K. Aygün, E. Michielssen, Analysis of transient electromagnetic scattering phenomena using a two-level plane wave time-domain algorithm, IEEE Trans. Antennas Propag. 48 (4) (2000) 510–523.
[2] A.E. Yılmaz, J.-M. Jin, E. Michielssen, D.S. Weile, A fast Fourier transform accelerated marching-on-in-time algorithm for electromagnetic analysis, Electromagnetics 21 (2001) 181–197.
[3] T. Abboud, J.-C. Nédélec, J. Volakis, Stable solution of the retarded potential equations, in: Proc. 17th ACES Conf., Monterey, CA, 2001, pp. 146–151.
[4] X. Wang, R.A. Wildman, D.S. Weile, P. Monk, A finite difference delay modeling approach to the discretization of the time domain integral equations of electromagnetics, IEEE Trans. Antennas Propag. 56 (8) (2008) 2442–2452.
[5] Y. Shi, M.-Y. Xia, R.-S. Chen, E. Michielssen, M. Lu, Stable electric field TDIE solvers via quasi-exact evaluation of MOT matrix elements, IEEE Trans. Antennas Propag. 59 (2) (2011) 574–585.
[6] A.J. Pray, N.V. Nair, B. Shanker, Stability properties of the time domain electric field integral equation using a separable approximation for the convolution with the retarded potential, IEEE Trans. Antennas Propag. 60 (8) (2012) 3772–3781.
[7] E. van 't Wout, D.R. van der Heul, H. van der Ven, C. Vuik, The influence of the exact evaluation of radiation fields in finite precision arithmetic on the stability of the time domain integral equation method, IEEE Trans. Antennas Propag. 61 (12) (2013) 6064–6074.
[8] F.P. Andriulli, K. Cools, F. Olyslager, E. Michielssen, Time domain Calderón identities and their application to the integral equation analysis of scattering by PEC objects Part II: Stability, IEEE Trans. Antennas Propag. 57 (8) (2009) 2365–2375.
[9] P.J. Davies, D.B. Duncan, On the behaviour of time discretisations of the electric field integral equation, Appl. Math. Comput. 107 (2000) 1–26.
[10] S.J. Dodson, S.P. Walker, M.J. Bluck, Implicitness and stability of time domain integral equation scattering analyses, ACES J. 13 (1998) 291–301.
[11] D.S. Weile, G. Pisharody, N.-W. Chen, B. Shanker, E. Michielssen, A novel scheme for the solution of the time-domain integral equations of electromagnetics, IEEE Trans. Antennas Propag. 52 (1) (2004) 283–295.
[12] E. van 't Wout, D.R. van der Heul, H. van der Ven, C. Vuik, Design of temporal basis functions for time domain integral equation methods with predefined accuracy and smoothness, IEEE Trans. Antennas Propag. 61 (1) (2013) 271–280.
[13] B. Shanker, M. Lu, J. Yuan, E. Michielssen, Time domain integral equation analysis of scattering from composite bodies via exact evaluation of radiation fields, IEEE Trans. Antennas Propag. 57 (5) (2009) 1506–1520.
[14] T. Ha-Duong, On retarded potential boundary integral equations and their discretisations, in: Topics in Computational Wave Propagation, in: Lecture Notes in Computational Science and Engineering, vol. 31, Springer, Berlin, 2003, pp. 301–336.
[15] M. Costabel, Time-dependent problems with the boundary integral equation method, in: Encyclopedia of Computational Mechanics, 2004, pp. 703–721.
[16] I. Terrasse, Résolution mathématique et numérique des équations de Maxwell instationnaires par une méthode de potentiels retardés (Ph.D. thesis), École Polytechnique, Palaiseau, 1993.
[17] A. Bamberger, T.H. Duong, Formulation variationnelle espace-temps pour le calcul par potentiel retardé de la diffraction d'une onde acoustique, Math. Methods Appl. Sci. 8 (1) (1986) 405–435. and 598–608.
[18] J. Ballani, L. Banjai, S. Sauter, A. Veit, Numerical solution of exterior Maxwell problems by Galerkin BEM and Runge–Kutta convolution quadrature, Numer. Math. 123 (4) (2013) 643–670.
[19] E. van 't Wout, D.R. van der Heul, H. van der Ven, C. Vuik, A provably stable MoT scheme based on quadratic spline basis functions, in: Proc. IEEE Antennas Propag. Soc. Int. Symp., Chicago, IL, 2012.
[20] G.C. Hsiao, R.E. Kleinman, Mathematical foundations for error estimation in numerical solutions of integral equations in electromagnetics, IEEE Trans. Antennas Propag. 45 (3) (1997) 316–328.
[21] P.A. Raviart, J.M. Thomas, A mixed finite element method for 2-nd order elliptic problems, in: Mathematical Aspects of Finite Element Methods, Springer, Berlin, 1977, pp. 292–315.
[22] S.M. Rao, D.R. Wilton, A.W. Glisson, Electromagnetic scattering by surfaces of arbitrary shape, IEEE Trans. Antennas Propag. 30 (3) (1982) 409–418.
[23] K. Cools, F.P. Andriulli, E. Michielssen, A Calderón multiplicative preconditioner for the PMCHWT integral equation, IEEE Trans. Antennas Propag. 59 (12) (2011) 4579–4587.
[24] P.J. Davies, D.B. Duncan, Convolution-in-time approximations of time domain boundary integral equations, SIAM J. Sci. Comput. 35 (1) (2013) 43–61.
[25] A. Geranmayeh, W. Ackermann, T. Weiland, Temporal discretization choices for stable boundary element methods in electromagnetic scattering problems, Appl. Numer. Math. 59 (2009) 2751–2773.
[26] T. Ha-Duong, B. Ludwig, I. Terrasse, A Galerkin BEM for transient acoustic scattering by an absorbing obstacle, Internat. J. Numer. Methods Engrg. 57 (2003) 1845–1882.
[27] G. Manara, A. Monorchio, R. Reggiannini, A space–time discretization criterion for a stable time-marching solution of the electric field integral equation, IEEE Trans. Antennas Propag. 45 (3) (1997) 527–532.
[28] E. van 't Wout, Stability, accuracy, and robustness of the time domain integral equation method for radar scattering analysis (Ph.D. thesis), Delft University of Technology, Delft, 2013.